Molecular Therapy
Methods & Clinical Development
Original Article

Traceless Targeting and Isolation of Gene-Edited Immortalized Keratinocytes from Epidermolysis Bullosa Simplex Patients

Magomet Aushev,[1] Ulrich Koller,[2] Claudio Mussolino,[3,4] Toni Cathomen,[3,4,5] and Julia Reichelt[2]

[1]Wellcome Trust Centre for Mitochondrial Research, Institute of Genetic Medicine, Biomedicine West Wing, Centre for Life, Times Square, Newcastle upon Tyne NE1 3BZ, UK; [2]EB House Austria, Research Program for Molecular Therapy of Genodermatoses and Department of Dermatology, University Hospital of the Paracelsus Medical University Salzburg, 5020 Salzburg, Austria; [3]Institute for Transfusion Medicine and Gene Therapy, Medical Center - University of Freiburg, Hugstetter Strasse 55, 79106 Freiburg, Germany; [4]Center for Chronic Immunodeficiency, Medical Center - University of Freiburg, Breisacher Strasse 115, 79106 Freiburg, Germany; [5]Faculty of Medicine, University of Freiburg, 79106 Freiburg, Germany

Epidermolysis bullosa simplex (EBS) is a blistering skin disease caused by dominant-negative mutations in either *KRT5* or *KRT14*, resulting in impairment of keratin filament structure and epidermal fragility. Currently, nearly 200 mutations distributed across the entire length of these genes are known to cause EBS. Genome editing using programmable nucleases enables the development of ex vivo gene therapies for dominant-negative genetic diseases. A clinically feasible strategy involves the disruption of the mutant allele while leaving the wild-type allele unaffected. Our aim was to develop a traceless approach to efficiently disrupt *KRT5* alleles using TALENs displaying unbiased monoallelic disruption events and devise a strategy that allows for subsequent screening and isolation of correctly modified keratinocyte clones without the need for selection markers. Here we report on TALENs that efficiently disrupt the *KRT5* locus in immortalized patient-derived EBS keratinocytes. Inactivation of the mutant allele using a TALEN working at sub-optimal levels resulted in restoration of intermediate filament architecture. This approach can be used for the functional inactivation of any mutant keratin allele regardless of the position of the mutation within the gene and is furthermore applicable to the treatment of other inherited skin disorders.

INTRODUCTION

Keratinopathies, such as epidermolysis bullosa simplex (EBS), epidermolytic ichthyosis (EI), and pachyonychia congenita (PC), are a group of inherited skin disorders mostly resulting from dominant-negative mutations in genes encoding keratins. Keratins are cytoskeletal proteins expressed in pairs that form heteropolymeric intermediate filaments (IFs), which protect cells from mechanical stress.[1] EBS, which is characterized by intraepidermal blistering after mechanical stress, is due to approximately 110 and 80 mutations in the keratin 5 (*KRT5*) and keratin 14 (*KRT14*) genes, respectively.[2] Keratin 5 (K5), a type II IF protein, and K14, a type I IF protein, are expressed in the basal layer of the epidermis,[3] which is home to epidermal stem cells responsible for tissue regeneration and repair.[4] Depending on the location within the genes, mutations in *KRT5* or *KRT14* cause different severity subtypes of EBS.[5,6] The mutant keratins polymerize with wild-type (WT) keratins into abnormal filaments that collapse upon mild mechanical stress, forming aggregates resulting in cytolysis and skin blistering.[7,8] The impairment of IF structure and aggregate formation upon stress can also be seen in cultured keratinocytes from EBS patients.[9–11] There is no cure for EBS and other keratinopathies, and current treatments focus on wound management and alleviating symptoms to improve the patient's quality of life.

One strategy for the treatment of dominant keratinopathies is the elimination of the mutant keratin in epidermal keratinocytes. It is known that keratins are expressed from both alleles and that one functioning allele is sufficient to maintain a structurally stable epidermis.[12–14] The use of small interfering RNA (siRNA) has shown promise in pre-clinical and clinical studies for EBS and PC.[15–18] However, siRNA cannot fully suppress gene expression and may have poor specificity.[19,20] Additionally, such an approach would not provide a permanent cure, and for successful in vivo application, an efficient and non-invasive delivery method is needed.[21]

An attractive alternative that would provide a permanent cure relies on the use of programmable nucleases such as zinc-finger nucleases (ZFNs), transcription activator-like effector nucleases (TALENs), and RNA-guided nucleases (RGNs) derived from the bacterial CRISPR-Cas system. These platforms have revolutionized genetic engineering and allow for the introduction of precise changes to specific sequences within a genome, showing great potential for the treatment of monogenic diseases.[22,23] By introducing DNA double-strand

Received 31 January 2017; accepted 30 June 2017;
http://dx.doi.org/10.1016/j.omtm.2017.06.008.

Correspondence: Julia Reichelt, EB House Austria, Research Program for Molecular Therapy of Genodermatoses and Department of Dermatology, University Hospital of the Paracelsus Medical University Salzburg, 5020 Salzburg, Austria.
E-mail: j.reichelt@salk.at

breaks (DSBs), programmable nucleases are able to activate endogenous repair machinery, resulting in gene disruption via non-homologous end joining (NHEJ) or gene correction via homology-directed repair (HDR) in the presence of a donor template.[24] We hypothesize that gene editing can be used to eliminate the mutant protein by disrupting the mutant allele while leaving the WT allele intact. EBS can thus serve as a model for the development of gene therapy approaches for this type of dominant-negative diseases. Furthermore, for several reasons, such an approach has a high potential to be translated into the clinic. First, the skin is accessible. Second, the epidermis hosts epidermal stem cells that can be grown in culture. Third, these stem cells have the rare ability among adult stem cells to grow clonally ex vivo while maintaining their stem cell capabilities.[25] This property allows the expansion of large numbers of keratinocytes from small skin biopsies. Expanded keratinocytes cannot only serve for the autologous treatment of third-degree burns, a technique that has been widely used for more than 30 years,[26,27] but have, in addition, been successfully used for combined gene and cell therapies.[28,29]

Previously, we have shown that ZFNs can be used to efficiently inactivate a transgene in murine epidermal stem cells without affecting stem cell characteristics such as self-renewal and differentiation.[30] The therapeutic effect of the epidermal stem cell strategy depends on the quality of the cells used for transplantation because only self-renewing stem cells sustain long-term skin regeneration.[31,32] Culturally stressed epidermal stem cells may differentiate,[33,34] possibly resulting in early graft loss. Culture stress may result from extended growth in culture and the use of selective methods such as fluorescence-activated cell sorting (FACS) and, possibly, antibiotic selection.[33] We therefore aimed to develop an approach for the screening and isolation of edited keratinocytes without the use of selection markers, minimizing culture stress and permitting the isolation of keratinocytes with desired changes.

A straightforward strategy would be the use of engineered nucleases targeting the disease-causing point mutations for allele-specific inactivation. However, this is difficult to implement for clinical translation because, for every single dominant-negative mutation, novel programmable nucleases with varying efficiencies and specificities would have to be designed and thoroughly validated. Although the simplicity of engineering behind the CRISPR/Cas9 system, along with highly specific Cas9 variants, may overcome this issue,[35] the number of mutations that can be targeted is restricted by the protospacer adjacent motif (PAM) sequence.[36] Furthermore, several of the known point mutations are not suitable for this strategy because targeting certain regions of the coding sequence may result in evasion of nonsense-mediated mRNA decay (NMD) and expression of a truncated protein rather than elimination of protein expression. An alternative strategy that can be used for all dominant-negative mutations and decreases the probability of producing truncated proteins is based on non-allele-specific targeting of the 5′ end of a coding sequence using a nuclease that displays unbiased monoallelic gene disruption events. Because of unbiased targeting of a non-allele-specific nuclease, a subset of cells treated with this nuclease will contain frameshifting indel mutations (small insertions or deletions) only on the mutant allele. These cells can then be identified using a screening approach and clonally expanded for clinical use. We sought to use TALENs because they combine high cleavage activity with high specificity.[37,38] TALENs function as dimers, and their activity depends on the spacer length between the monomer binding sites.[37,38] We therefore assessed four TALEN pairs that target binding sites with spacers of 12–15 bp to identify TALENs displaying high monoallelic gene disruption.

The present study describes a novel approach for the screening and clonal expansion of keratinocytes edited with a TALEN of lower activity that displayed unbiased monoallelic gene disruption. Disruption of the mutant *KRT5* allele in immortalized patient-derived keratinocyte clones eliminated structural abnormalities in IFs and formation of IF aggregates upon stress. Therefore, a less active engineered nuclease combined with screening and clonal expansion can be used for the development of ex vivo gene therapies of autosomal dominant keratinopathies, such as EBS, regardless of the position of the mutation within the gene.

RESULTS

Targeting of the *KRT5* Locus

We generated six TALEN monomers to target two distinct sites in exon 1 of *KRT5* (Figure 1A) and tested them in pairs for their activity in immortalized normal and EBS human keratinocytes with missense mutations in exon 2 and exon 7 (Figure 1B) using an optimized screening approach (Figure 1C). The screening approach focused on determining the gene disruption efficiencies, followed by clonal expansion and subsequent screening of transfected clones. The edited clones were then transferred to a larger culture vessel for additional expansion, followed by further analysis. TALENs 1A-2 and 1B-2 were composed of different left monomers, "1A" or "1B," and a common right monomer, "2." These two TALEN pairs targeted the same region with a difference in monomer spacing of 12 bp and 14 bp, respectively. Similarly, TALENs 3-4A and 3-4B had a common left monomer, 3," and targeted the same region with a monomer spacing of 13 bp and 15 bp, respectively. The presence of CpG dinucleotides within the TALEN target sites was noted because potentially methylated cytosines might affect TALEN binding (Figure S1).[39–41]

Gene disruption efficiencies of TALENs were assessed by the detection of indels resulting from imperfect repair via NHEJ using the T7E1 assay. Cultured immortalized normal (NKc21) and EBS (EB11 and EB21) keratinocytes were cotransfected with two plasmids, each encoding a TALEN monomer. Activity of all four TALEN pairs was detected in NKc21, EB11, and EB21 cells (Figure 2). In immortalized normal human keratinocytes (NKc21) transfected with TALEN 1A-2, 36% of alleles contained indels. The same TALEN induced indels of 25% and of 18% in EB11 and EB21, respectively. A consistent lower activity was observed in cells transfected with TALEN pairs 1B-2 (29% in NKc21, 22% in EB11, and 16% in EB21), 3-4A (22% in NKc21, 21% in EB11, and 16% in EB21), and 3-4B (18% in NKc21, and 6% in EB11 and EB21) compared with cells transfected with TALEN 1A-2, with TALEN 3-4B displaying the lowest levels of NHEJ.

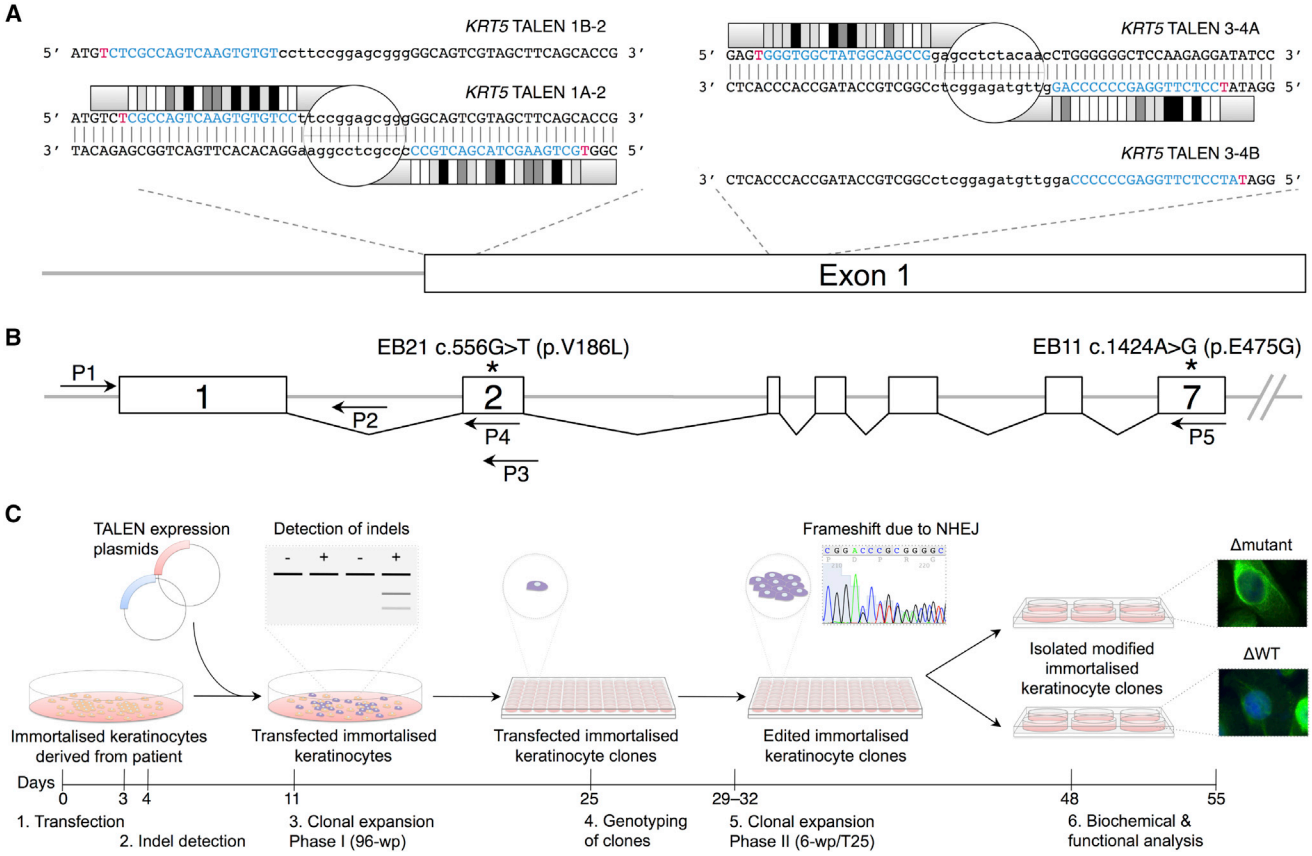

Figure 1. TALEN Targeting Strategy for *KRT5*

(A) TALENs were designed to target exon 1 of *KRT5*. The target sites of TALENs 1A-2 (12-bp spacer, lowercase), 1B-2 (14-bp spacer, lowercase), 3-4A (13-bp spacer, lowercase), and 3-4B (15-bp spacer, lowercase) and location within exon 1 are shown. TALEN binding sites (blue) with thymidine position 0 (red) are indicated. Dimerized FokI nuclease domains are shown (white). (B) Schematic of the *KRT5* gene with exons 1–7 (white boxes) and primers (arrows) used for direct PCR or allele-specific PCR. Shown are reverse primers (P2 for EB11 and P3 for EB21) used for direct PCR screening. Reverse primers (P4 and P5) that bound to the point mutations were used to distinguish the wild-type and mutant alleles. Point mutations in EB21 and EB11 are located in exon 2 and exon 7 (asterisks), respectively. (C) Timeline of the genome editing approach with individual steps. The approach involves transient transfection of immortalized keratinocytes using TALEN expression constructs, detection of indels (T7E1 assay), clonal expansion (phase I), genotyping of clones (sequencing of TALEN target sites via direct PCR and individual alleles via allele-specific PCR), and further expansion (phase II), followed by biochemical and functional analysis of the keratin intermediate filaments (immunofluorescence, live-cell imaging, and western blotting). For the production of pure clones, a waiting period of 7 days after transfection was applied to ensure that all traces of TALENs were removed prior to clonal expansion. Isolation of edited clones following full analysis can be achieved after 8 weeks.

We next tested whether the TALENs could achieve similar gene disruption efficiencies in primary human keratinocytes isolated from a healthy donor. Primary human keratinocytes were edited by all four TALEN pairs with efficiencies similar to EB21 (Figure 2). The different levels of NHEJ detected between the cell lines were due to varying transfection efficiencies as shown by flow cytometric analysis (Figure S2). Lower transfection efficiency was observed for the EBS lines (55% for EB11 and 47% for EB21) and primary keratinocytes (43%) compared with the normal keratinocyte line (68% for NKc21). Analysis of transfection efficiencies using flow cytometry data of primary keratinocytes showed the presence of three populations that differed in size, with two smaller populations containing 47% and 48% transfected ($EGFP^+$) cells, whereas only 25% of the larger cells were transfected (Figure S3). This result suggests that the overall decreased transfection efficiency of primary keratinocytes was due to the presence of larger (i.e., terminally differentiated) postmitotic keratinocytes abundant in primary cultures,[42] which are known to be more difficult to transfect. In summary, analysis of four different TALEN pairs in patient-derived keratinocytes showed varying activities.

Screening for Monoallelic Edited Keratinocyte Clones

To determine the number of edited clones, immortalized EBS keratinocytes transfected with the different TALEN pairs were clonally expanded, and TALEN target sites were analyzed for indel formation using direct PCR and sequencing. Screening of keratinocyte clones revealed the presence of distinct indels at the TALEN target sites (Figure 3A; Figure S4). The most common indels observed were deletions, and the majority of the NHEJ events resulted in frameshifts.

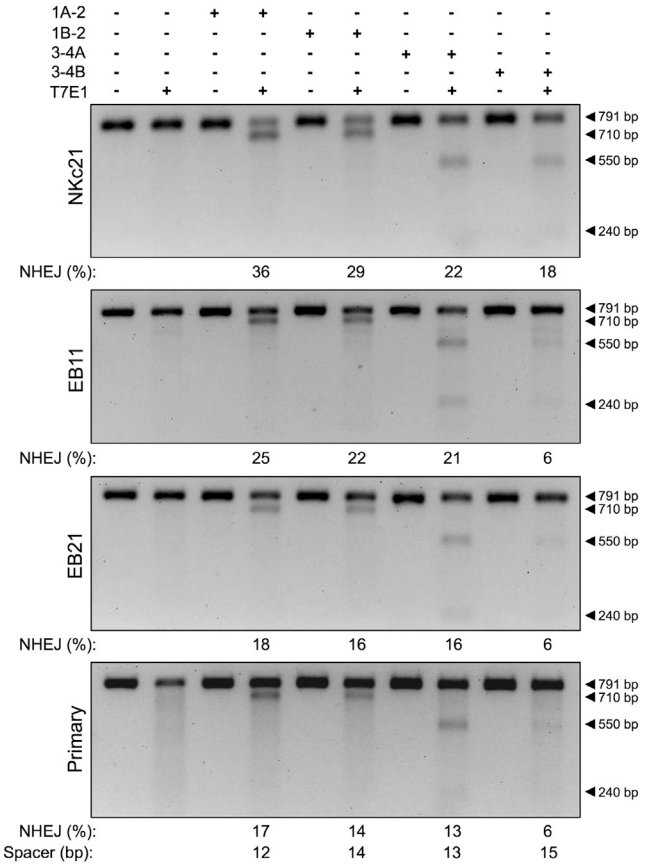

Figure 2. Efficient TALEN-Mediated Disruption of the *KRT5* Locus in Human Keratinocytes

NKc21, EB11, EB21, and primary keratinocytes were transfected with expression plasmids encoding the indicated TALEN (1A-2, 12-bp spacer; 1B-2, 14-bp spacer; 3-4A, 13-bp spacer; 3-4B, 15-bp spacer). Genomic DNA was extracted 1 week after transfection and subjected to PCR amplification of the target site, followed by T7E1 assay. The spacer lengths between each TALEN monomer and the extent of cleavage are indicated below. Arrowheads indicate the position of the cleaved and uncleaved products with the corresponding sizes.

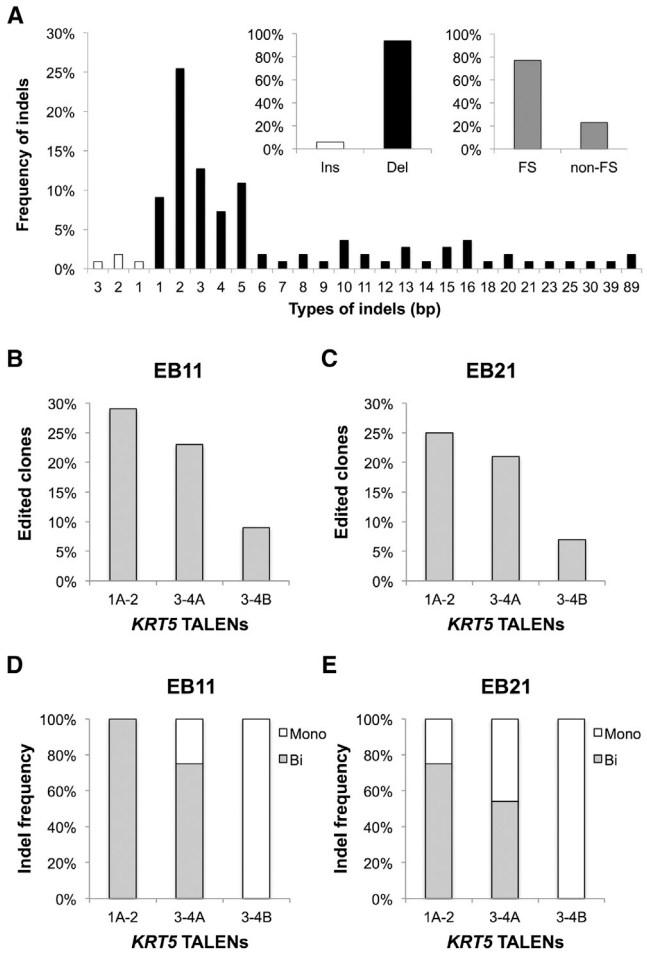

Figure 3. Efficient TALEN-Mediated Editing of *KRT5* in Immortalized Human Keratinocytes

(A) Sequencing data of edited keratinocyte clones summarizing the types of indels observed; deletions (black) and insertions (white) are shown. Shown are the levels of total insertions (white) and deletions (black) observed; 6% insertions, 94% deletions. Also shown are the levels of frameshift (FS) and non-frameshift (non-FS) NHEJ events; 77% FS, 23% non-FS. (B and C) The percentages of edited (B) EB11 clones transfected with TALEN 1A-2 (29%, n = 34), 3-4A (23%, n = 71), or 3-4B (9%, n = 22) and (C) EB21 clones transfected with TALEN 1A-2 (25%, n = 16), 3-4A (21%, n = 124), or 3-4B (7%, n = 30). (D and E) Allelic disruption frequencies in (D) EB11 clones edited by TALEN 1A-2 (100% bi, n = 10), 3-4A (75% bi and 25% mono, n = 16), or 3-4B (100% mono, n = 2) and (E) EB21 clones edited by TALEN 1A-2 (75% bi and 25% mono, n = 4), 3-4A (54% bi and 46% mono, n = 26), or 3-4B (100%, n = 2). Edited clones with bialleleic (gray) and monoallelic (white) modifications are indicated.

Interestingly, two independent indel profiles were observed in the same target site of some clones edited with TALEN 1A-2 or 3-4A (Figure S4), suggesting the occurrence of multiple NHEJ events in the same cell that were generated from repeated TALEN binding and cleavage. Indels were detected in 29% of EB11 clones treated with TALEN 1A-2 (Figure 3B). Similarly, indels were detected in 25% of EB21 clones treated with TALEN 1A-2 (Figure 3C). Because of the similarity in the levels of gene disruption in immortalized keratinocytes treated with TALEN 1B-2 or 3-4A, cells treated with TALEN 1B-2 were not seeded for clonal expansion and further analysis. TALEN 3-4A resulted in editing frequencies of 23% in EB11 and 21% in EB21 clones, whereas TALEN 3-4B induced indel formation of 9% and 7% in EB11 and EB21 clones, respectively.

TALEN 1A-2 produced a surprisingly high number of biallelic modifications in both EB11 and EB21 clones (Figures 3D and 3E). Both biallelic and monoallelic modifications were seen in EB11 and EB21 clones transfected with TALEN 3-4A. Interestingly, the ratio of biallelic to monoallelic modifications between EB11 and EB21 clones varied. Edited EB11 clones exhibited 75% of biallelic and 25% monoallelic gene disruption, whereas EB21 clones exhibited 54% biallelic and 46% monoallelic disruption. All EB11 and EB21 clones edited with TALEN 3-4B showed only monoallelic indel formation. Clones edited on a single allele were further analyzed by allele-specific PCR

EB11 and EB21 monoallelic clones

Clone ID	Line	Allele	Target site	Indel	TALEN
-	WT	-	5'-GTCTCGCCAGTCAAGTGTGTCC ttccggagcggg GGCAGTCGTAGCTTCAGCACCG-3'	-	1A-2
A6	EB21	N/D	5'-GTCTCGCCAGTCAAGTGTGTCC ttccgg.....gg GGCAGTCGTAGCTTCAGCACCG-3'	Δ4 bp	1A-2
-	WT	-	5'-GAGTGGGTGGCTATGGCAGCCG gagcctctacaac CTGGGGGGCTCCAAGAGGATAT-3'	-	3-4A
B7	EB21	WT	5'-GAGTGGGTGGCTATGGCAGCCG gagc.....tacaac CTGGGGGGCTCCAAGAGGATAT-3'	Δ3 bp	3-4A
B10	EB21	WT	5'-GAGTGGGTGGCTATGGCAGCCG gagcct.....acaac CTGGGGGGCTCCAAGAGGATAT-3'	Δ2 bp	3-4A
B31	EB21	WT	5'-GAGTGGGTGGCTATGGCAGCCG gagcctct.....c CTGGGGGGCTCCAAGAGGATAT-3'	Δ4 bp	3-4A
B73	EB21	WT	5'-GAGTGGGTGGCTATGGCAGCCG gagcctc.....caac CTGGGGGGCTCCAAGAGGATAT-3'	Δ2 bp	3-4A
B77	EB21	Mut	5'-GAGTGGGTGGCTATGGCAGCCG gagcct.....acaac CTGGGGGGCTCCAAGAGGATAT-3'	Δ2 bp	3-4A
B92	EB21	Mut	5'-GAGTGGGTGGCTATGGCAGCCG gagcctc...acaac CTGGGGGGCTCCAAGAGGATAT-3'	Δ1 bp	3-4A
B99a	EB21	WT	5'-GAGTGGGTGGCTATGGCAGCCG gagcct.....acaac CTGGGGGGCTCCAAGAGGATAT-3'	Δ2 bp	3-4A
B102	EB21	WT	5'-GAGTGGGTGGCTATGGCAGCCG gagcctc.....caac CTGGGGGGCTCCAAGAGGATAT-3'	Δ2 bp	3-4A
B105	EB21	N/D	5'-GAGTGGGTGGCTATGGCAGCCG gagcc.....caac CTGGGGGGCTCCAAGAGGATAT-3'	Δ4 bp	3-4A
B126b	EB21	WT	5'-GAGTGGGTGGCTATGGCAGCCG gag.....tctacaac CTGGGGGGCTCCAAGAGGATAT-3'	Δ2 bp	3-4A
B133	EB21	WT	5'-GAGTGGGTGGCTATGGCAGCCG gagcc.....tacaac CTGGGGGGCTCCAAGAGGATAT-3'	Δ2 bp	3-4A
B136b	EB21	WT	5'-GAGTGGGTGGCTATGGCAGCCG gagcctc..... .....CCAAGAGGATAT-3'	Δ16 bp	3-4A
E18	EB11	N/D	5'-GAGTGGGTGGCTATGGCAGCCG gagcctc.....aac CTGGGGGGCTCCAAGAGGATAT-3'	Δ3 bp	3-4A
E26	EB11	Mut	5'-GAGTGGGTGGCTATGGCAGCCG gag.....tctacaac CTGGGGGGCTCCAAGAGGATAT-3'	Δ2 bp	3-4A
E62	EB11	WT	5'-GAGTGGGTGGCTATGGCAGCCG gagcct...tacaac CTGGGGGGCTCCAAGAGGATAT-3'	Δ1 bp	3-4A
E74	EB11	Mut	5'-GAGTGGGTGGCTATGGCAGCCG gagcct.....acaac CTGGGGGGCTCCAAGAGGATAT-3'	Δ2 bp	3-4A
-	WT	-	5'-GAGTGGGTGGCTATGGCAGCCG gagcctctacaacct GGGGGGCTCCAAGAGGATATCC-3'	-	3-4B
21	EB21	WT	5'-GAGTGGGTGGCTATGG..... .....tacaacct GGGGGGCTCCAAGAGGATATCC-3'	Δ13 bp	3-4B
43	EB21	WT	5'-GAGTGGGTGGCTATGGCAGCCG gagcctc.....caacct GGGGGGCTCCAAGAGGATATCC-3'	Δ2 bp	3-4B
7	EB11	Mut	5'-..... .....acaacct GGGGGGCTCCAAGAGGATATCC-3'	Δ30 bp	3-4B
8	EB11	WT	5'-GAGTGGGTGGCTATGGCAGCCG gcgcctc.....acct GGGGGGCTCCAAGAGGATATCC-3'	Δ4 bp	3-4B

Figure 4. EB11 and EB21 Monoallelic Clones

Sequencing summary of EB11 (n = 6) and EB21 (n = 15) clones with monoallelic modifications generated by TALEN 1A-2, 3-4A, or 3-4B. Target sites (blue) of TALENs 1A-2, 3-4A, or 3-4B are shown, with thymidine position 0 (red) indicated. N/D, not determined.

and sequencing. All of the edited EB11 clones showed an equal ratio of allelic disruption frequency (Figure 4). In EB21 clones, however, a preference for the WT allele with a disruption ratio of 4:1 was observed; i.e., modification of four WT alleles for every mutant allele. In summary, screening of keratinocytes clones identified clones with corrective modifications and TALEN pairs displaying monoallelic gene disruption.

Editing of Individual Alleles Results in Alterations in Intermediate Filament Structure

To confirm that editing of the *KRT5* locus resulted in changes in IF stability, we analyzed two randomly selected EB11 and EB21 clones with indels on either the mutant or the WT allele resulting in frameshifts (Figure 4). Two EB11 clones, one with a 2-bp deletion on the mutant allele (EB11 Δmut clone, E26) and one with a 4-bp deletion on the WT allele (EB11 ΔWT clone, 8), resulting in the induction of premature translation-termination codons (PTCs) in two different frames, were analyzed by immunofluorescence. Similarly, two EB21 clones, one with a 2-bp deletion on the mutant allele (EB21 Δmut clone, B77) and one with a 2-bp deletion on the WT allele (EB21 ΔWT clone, 43), were analyzed by immunofluorescence. Unmodified EB11 and EB21 lines and isolated unmodified clones were used as controls.

Prior to immunofluorescence, keratin filament stability was challenged by the application of thermal or hypo-osmotic stress. Following stress, both immortalized normal and EBS keratinocytes rounded up, suggesting filament disassembly. Additional changes occurred in the EBS cells, indicating reduced resilience of the IF cytoskeleton. Immunofluorescence staining for K5 in EB11 cells showed the presence of cytoplasmic keratin aggregates localized mostly to the cell periphery in 30.3% ± 4.1% of unstressed, 37.3% ± 5.2% of thermally stressed, and 44.5% ± 3.7% of osmotically stressed cells, confirming the severity of the phenotype (Figure 5). Staining of an unmodified EB11 clone showed collapse of filaments forming a shell around the nucleus rather than keratin aggregates in the cell periphery. Analysis of the EB11 Δmut clone E26 showed homogeneous distribution of IF throughout the cytoplasm and absence of keratin aggregates or collapsed filaments around the nucleus. The cells appeared morphologically normal, suggesting that inactivation of the mutant allele restored IF stability. In contrast, EB11 ΔWT clone 8 showed a more severe phenotype with absence of normal filaments and the presence of a high number of keratin aggregates of various sizes distributed throughout the cytoplasm in 98.6% ± 1.4% of unstressed, 98.1% ± 1.9% of thermally stressed, and all osmotically stressed cells. Additionally, large clumps of collapsed keratin filaments adjacent to the nucleus were observed. Immunofluorescence staining for K5 in EB21 cells did not show the presence of keratin aggregates, which is consistent with the moderate disease phenotype associated with the underlying mutation (Figure S5). Staining of the unmodified EB21 clone showed the absence of a homogeneous cytoskeleton. Similarly to EB11 Δmut clone E26, analysis of EB21 Δmut clone B77 showed an overall improved appearance of the cytoskeleton in all cells. Staining of EB21 ΔWT clone 43 showed the presence of keratin aggregates in only 5.6% ± 1.1% of thermally stressed and 4.8% ± 0.2% osmotically stressed cells. Immunofluorescence analysis of the edited EBS clones showed that

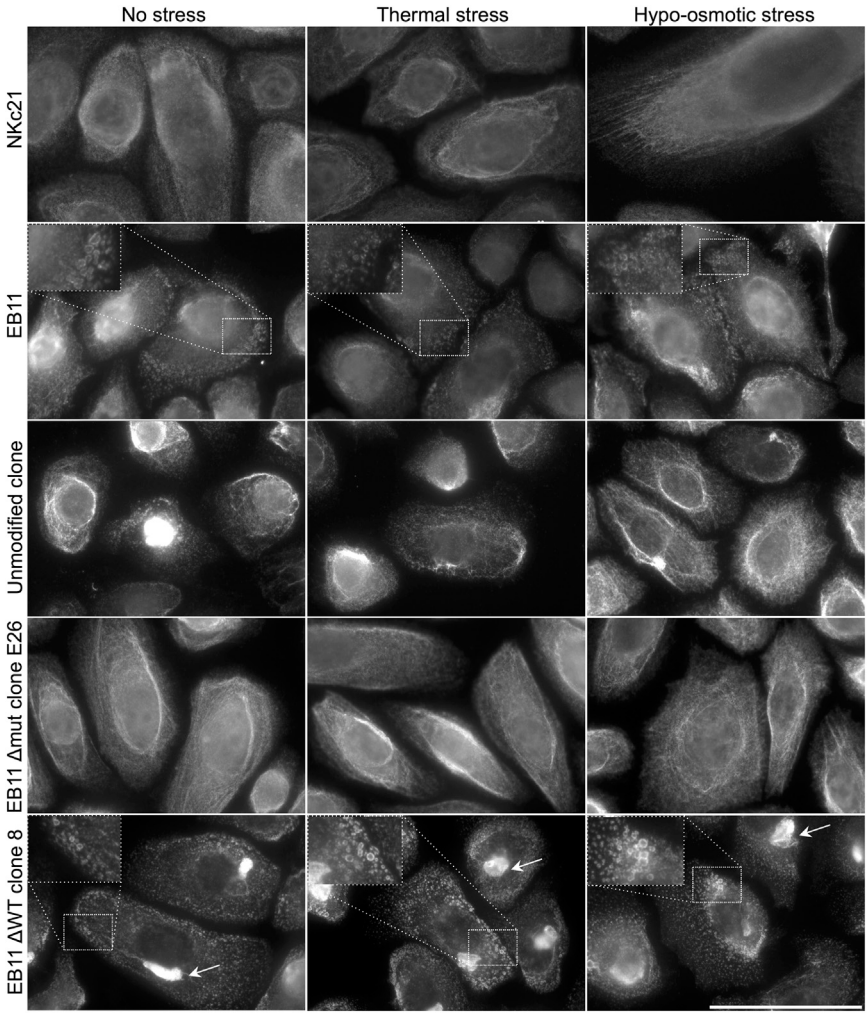

Figure 5. TALEN-Mediated Editing of *KRT5* in EB11 Cells Resulted in Changes to Keratin Intermediate Filament Stability

Immunofluorescence staining of K5 with and without thermal or hypo-osmotic stress in NKc21, EB11, the unmodified EB11 clone, EB11 Δmut clone E26, and EB11 ΔWT clone 8. Insets show higher magnifications of the framed areas. Keratin aggregates are indicated (white boxes). Large clumps of collapsed keratin filaments adjacent to the nucleus are indicated (white arrows). Scale bar, 50 μm.

inactivation of the mutant *KRT5* allele resulted in changes to IF distribution, suggesting restored filament stability. In contrast, inactivation of the WT allele resulted in exacerbation of IF abnormalities.

Clones were thermally stressed and visualized using fluorescent microscopy to observe changes in IF stability in real time (Figure 6A). Live-cell imaging was performed by transfecting clones with expression constructs coding for murine keratin 10 (K10) fused to EGFP (Figure 6B). The type I keratin K10 is normally not expressed in keratinocytes grown in culture (i.e., undifferentiated keratinocytes), but will, because of the promiscuity of keratins, integrate into any keratin filament, such as K5/K14 filaments, upon transfection into these cells. No aggregate formation was observed in NKc21 cells after the application of thermal stress (Figure 6C). However, real-time keratin aggregate formation and filament collapse were observed in EB11 cells after the application of thermal stress. In EB11 Δmut clone E26, no aggregate formation was detected in response to thermal stress, suggesting increased stability of keratin filaments. In contrast, EB11 ΔWT clone 8 revealed filament collapse into one single clump around the nucleus. No aggregate formation was observed in EB21 cells (Figure S6). EB21 Δmut B77 clone showed improvements to filament stability, whereas EB21 ΔWT clone 43 showed the presence of keratin aggregates in thermally stressed cells. Observed changes in IF stability and aggregate formation suggest that TALEN-mediated editing of the mutant or WT allele resulted in alleviation or aggravation of the EBS phenotype in vitro, respectively.

To determine whether editing of the *KRT5* locus resulted in reduction in K5, protein levels were analyzed using western blotting. Expression levels of K5 were unaltered in the EB11 and EB21 clones (Figures S7A and S7B) compared with the unedited lines, and truncated proteins were not detected. Interestingly, the EB21 line showed higher levels of K5 than NKc21 and EB11, suggesting polyploidy of chromosome 12, which is consistent with the 4:1 ratio of editing, sequencing, and imaging results.

An overview of the modification approach based on EB11 transfected with TALEN 3-4A showed that, of the total population, 5.6% (4 of 71) had monoallelic modifications, and about half of these clones were edited on the mutant allele, as expected from unbiased targeting (Table 1). Taking into account that only two-thirds of all NHEJ events would lead to a frameshift, ~2% of clones would contain a "therapeutic" modification. This is due to the high incidence of biallelic gene disruption. EB11 transfected with TALEN 3-4B, on the other hand, showed 9% (2 of 22) of clones with monoallelic disruption and, thus, 3% of clones potentially carrying a corrective modification.

Off-Target Analysis

An important factor in the successful application of designer nucleases in a clinical setting is specificity. We therefore assessed the off-target activity of each TALEN pair in the transfected EB11 and EB21 populations using a T7E1 assay. Assessment of a total of ten hetero- and homodimeric off-target sites (two to four per TALEN) showed undetectable off-target cleavage in both EB11 and EB21 (Figure S8). Although the T7E1 digestion patterns of some off-target

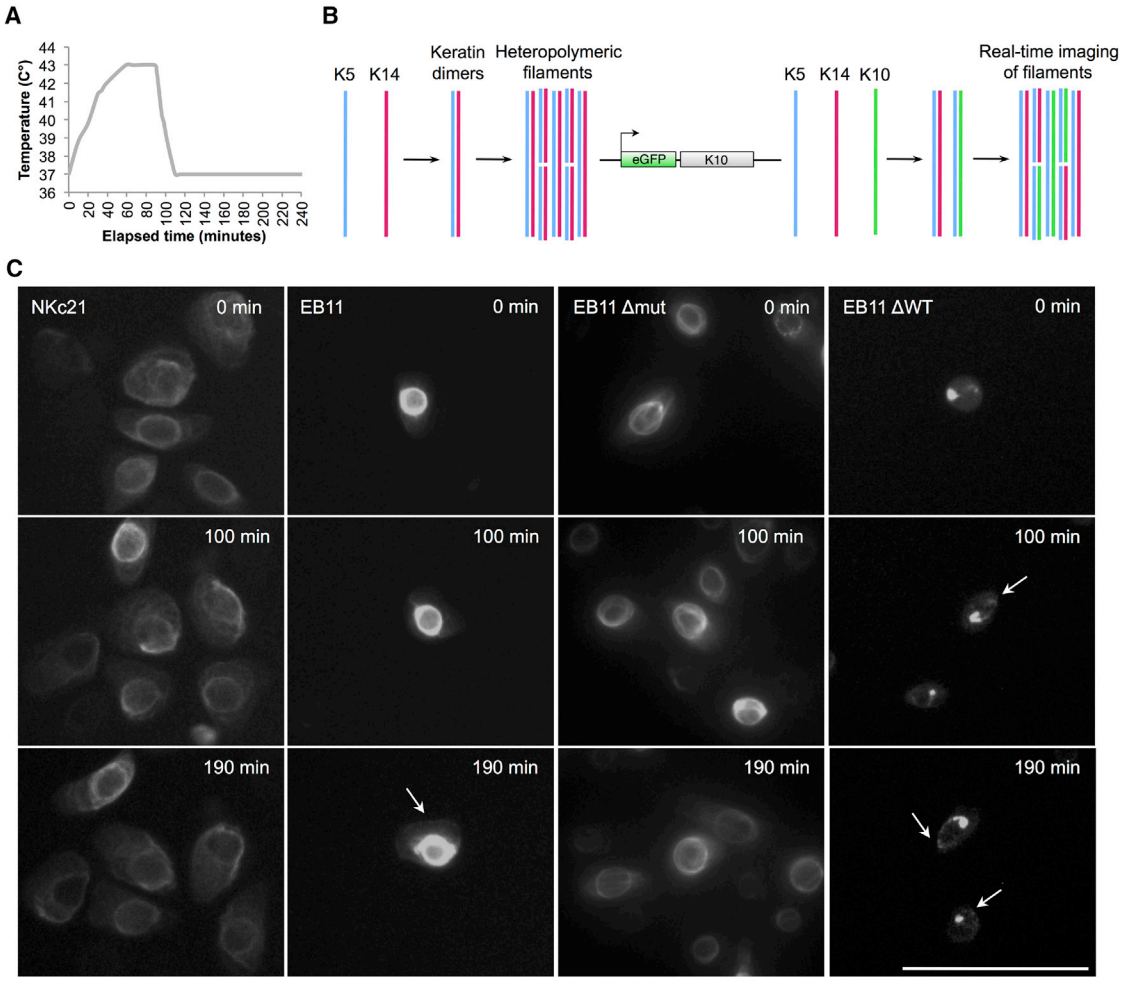

Figure 6. Live Visualization of Keratin Filament Stability in Edited EB11 Clones

(A) Thermal stress was applied for 30 min at 43°C. Cells were visualized for 4 hr before, during, and after stress. Photographs were taken every 5 min at four fixed positions for each cell line or clone. (B) K5, a type II intermediate filament, and K14, a type I, dimerize to form heteropolymeric intermediate filaments. K10, also a type I, can dimerize with K5 and be integrated into pre-existing filaments. Labeling of intermediate filaments can be achieved by introducing an EGFP-K10 fusion protein into the cells. (C) Live-cell imaging of NKc21, EB11, EB11 Δmut clone E26, and EB11 ΔWT clone 8 using EGFP-K10 labeling of keratin filaments. K10 will integrate into pre-existing keratin filaments made up of K5 and K14. Keratinocytes were transfected with constructs coding for an EGFP-K10 fusion protein and visualized using fluorescence microscopy. Keratin aggregate formation (white arrows) is indicated. Scale bar, 100 μm.

regions (OT-5, OT-8, OT-9, and OT-10) showed several DNA fragment sizes, including bands in the range of the predicted fragments, these were most likely not specific because exactly the same patterns were also present in the negative controls.

DISCUSSION

TALENs hold great potential for the development of ex vivo gene therapies for dominant-negative genetic diseases such as EBS. They enable targeting of stem cells and disruption of the mutant allele, thus providing a permanent cure. We describe an approach for screening and isolation of gene-edited immortalized human epidermal keratinocytes. With this approach, correctly modified clones can be identified in less than 1 month after transfection. The application of such an approach in combination with TALENs displaying unbiased monoallelic gene disruptions in a clinical setting is clinically relevant for several reasons. First, the approach relies on NHEJ, which is significantly more efficient than HDR, especially in primary human keratinocytes (~9% versus <1%).[43] Second, marker-dependent selection methods such as FACS or antibiotic treatment, which may leave marks in targeted cells and be a source of culture stress for epidermal stem cells, are avoided.[33] Third, epidermal stem cells can be cultured for at least 180 population doublings on feeder cells[44,45] or up to passage 20 using transforming growth factor β (TGF-β)/BMP inhibitors.[46] Human epidermal stem cells cultured on mouse feeder fibroblasts have been used for both cell and gene therapy,[26,28,29] and cultured autologous epidermal grafts

Table 1. Summary of the Clonal Analysis

Clones	TALEN	Analyzed	Modified	Biallelic	Monoallelic	WT	Mutant
EB11	1A-2	34	10	10	–	–	–
EB11	3-4A	71	16	12	4	1	2
EB11	3-4B	22	2	–	2	1	1
EB21	1A-2	16	4	3	1	–	–
EB21	3-4A	124	26	14	12	9	2
EB21	3-4B	30	2	–	2	2	–

that rely on mouse feeder layers have been approved by the Food and Drug Administration (FDA) (Epicel by Sanofi Biosurgery). Fourth, the fact that programmable nucleases are capable of targeting sites with several mismatches clearly shows that a clonal approach provides a higher degree of safety.[38,47] It allows the isolation, selection, and transplantation of safe and correctly modified keratinocyte clones from a mass culture.[48]

In our study, we describe traceless targeting of immortalized human epidermal keratinocytes using TALENs. We show that TALENs efficiently disrupted the *KRT5* locus in immortalized human epidermal keratinocytes, with 29% of clones showing indels. This is important because increasing the number of modified stem cell clones increases the number of potential candidates for transplantation. We observed similar or higher gene disruption efficiencies in immortalized patient-derived and primary keratinocytes than the previously reported efficiencies in primary fibroblasts from a patient with recessive dystrophic epidermolysis bullosa[47] or ZFN-mediated efficiencies in immortalized junctional epidermolysis bullosa keratinocytes.[43] Using clonally expandable cells, we were able to analyze TALEN-induced NHEJ events in single cells. We have previously described variations in gene disruption efficiencies of TALENs depending on linker and spacer lengths.[37,38] Here we observed that a TALEN with a 17-amino acid (aa) linker exhibited high efficiency of indel production on a target site with a short optimal spacer of 12 bp. This high cleavage activity was associated with a high frequency of biallelic gene disruption, which would be ideal for gene therapies where complete ablation of a gene is beneficial, such as the expression of *CCR5* in HIV-positive individuals.[49] In contrast, a TALEN recognizing a target site with a longer spacer of 13 bp or 15 bp exhibited lower activity, which was associated with more monoallelic gene disruption. Although the overall activity of the 3-4B TALEN pair (15 bp) was lower compared with TALEN 3-4A (13 bp), the absolute frequency of monoallelically modified clones was higher. In the case of EBS, where a functioning WT allele is essential, one could increase the probability of identifying clones with monoallelic modifications by designing TALENs with lower overall activity, but a systematic approach is needed to determine whether these observations remain true for all TALENs. Furthermore, we show that TALENs were able to target the *KRT5* locus with high specificity because no off-target cleavage was detected. This is consistent with the previously observed TALEN specificities.[38]

An alternative is to exploit a point mutation or a SNP to specifically target an allele. Efficient targeting of human keratinocytes for therapy is feasible; however, because of the importance of having as many viable epidermal stem cell clones as possible, it would be more strategic to use SNPs or point mutations to target individual alleles because the high specificity of TALENs permits that. However, this would be challenging and time-consuming to implement for 200 mutations in two genes. We only examined spacers of 12–15 bp as opposed to 20–22 bp because this was the highest peak of TALEN activity of the current architecture.[37,38] Interestingly, sequencing data from clones edited by TALEN 1A-2 or 3-4A suggest multiple consecutive NHEJ events, possibly because of repeated TALEN binding and cleavage. As previously shown,[38] TALENs of the Δ135/+17 architecture are active at a 10-bp spacer between monomers. A Δ2-bp deletion in the spacer of a TALEN originally designed with a 12-bp spacer (e.g., 1A-2) may thus permit a further increase in activity. Similarly, a TALEN originally designed with a 14-bp spacer (e.g., 3-4A) may also be active at the same target site when a Δ2 bp deletion is present.

Furthermore, we show that inactivation of the mutant *KRT5* allele resulted in elimination of structural abnormalities in IFs and formation of aggregates upon stress. No previous work has been done for EBS and other keratin disorders using programmable nucleases. Because of the low availability of primary cells from patient samples, we chose immortalized EBS keratinocytes as the model system to validate our approach. Furthermore, the two cell lines used were previously characterized and reported to show keratin aggregates in culture. Keratin aggregates are a direct indication of IF abnormalities and phenotype severity because there is a strict genotype-phenotype correlation.[5,6,10,11] Interestingly, EB21 cells were reported to show keratin aggregates in over 10% of stressed cells.[9] However, we only observed keratin aggregates in 5% of stressed cells in the EB21 ΔWT clone. Furthermore, we observed different frequencies of bi- and monoallelic targeting between EB11 and EB21, with TALEN targeting in EB21 clones showing a preference for the WT allele. Taken together with the observed higher levels of K5 expression, this suggests polyploidy for chromosome 12 in EB21. This is consistent with a previous study that reported tetraploidy in metaphase spreads of EB21 cells.[9] This highlights the importance of choosing the right model system. We observed no reduction in the expression levels of K5 in modified clones. This may be due to upregulation of gene expression from the WT allele.

Overall, our data support that TALENs are excellent tools for gene disruption and have high potential for clinical use. We describe a strategy that is based on a less active TALEN pair that can be used for unbiased monoallelic gene disruption in immortalized patient-derived keratinocytes, followed by screening and isolation of gene-edited immortalized keratinocytes without the use of selection markers. Importantly, inactivation of the mutant *KRT5* allele resulted in elimination of IF abnormalities. Together, these findings bring us a step closer to realizing a traceless ex vivo gene therapy for disorders resulting from dominant-negative mutations, such as EBS.

MATERIALS AND METHODS

Cell Culture and Transfection

Immortalized patient-derived EBS (EB11 and EB21) and healthy donor (NKc21) keratinocyte lines were cultured in EpiLife medium (Life Technologies) supplemented with human keratinocyte growth supplement (HKGS, Life Technologies) and penicillin/streptomycin/amphotericin (PSA) (100 U/mL penicillin, 100 μg/mL streptomycin, 0.25 μg/mL amphotericin B; Lonza). EB11 was originally derived from a patient with generalized severe EBS (formerly known as Dowling-Meara EBS, DM-EBS) resulting from a p.Glu475Gly substitution in exon 7.[11] EB21 was originally derived from a patient with moderate EBS (formerly known as Koebner-type EBS) resulting from a p.Val186Leu substitution in exon 2.[9] NKc21 is a normal keratinocyte line isolated from a healthy donor that was used as a control.[50] Primary human keratinocytes were isolated from adult foreskin samples normally discarded after surgical procedures and cultured in CnT-Prime medium (CELLnTEC) supplemented with PSA (Lonza). 3T3-J2 mouse fibroblast feeders were grown in DMEM with 4.5 g/L glucose and L-glutamine (Lonza) supplemented with 10% fetal bovine serum (FBS) (Sigma-Aldrich) and penicillin/streptomycin (PS) (100 U/mL penicillin and 100 μg/mL streptomycin, Lonza). Cells were maintained at 37°C in a 5% CO_2 atmosphere. Cells were cultured in 6-well plates and transfected at 50%–70% confluence with 3 μg of TALEN expression plasmids using 0.5 μL Xfect (Clontech) according to the manufacturer's instructions. Cells were cultured at 30°C for 3 days 4 hr after transfection as described previously.[51] For the assessment of transfection efficiency, cells were transfected with 3 μg of EGFP expression plasmids (Clontech). Cells were cultured at 37°C and analyzed for EGFP expression 48 hr after transfection.

Flow Cytometry

Flow cytometry was used to determine transfection efficiency and was carried out using BD FACSCanto II (BD Biosciences). Transfected keratinocytes were trypsinized and resuspended in PBS. EGFP fluorescence was measured using a BP 530/30 filter. BD FACSDiva software version 8.0 was used for analysis (BD Biosciences). EGFP (pEGFP-C1, Clontech) was used for the assessment of transfection efficiency.

TALEN Constructs

KRT5-specific TALENs were engineered via the Golden Gate assembly method[52] based on the 17-aa linker (Scaffold A4-NH) architecture of Mussolino et al.[37] as follows: left TALEN monomer (1A), HD NN HD HD NI NN NG HD NI NI NN NG NN NG NN NG HD HD; left TALEN monomer (1B), HD NG HD NN HD HD NI NN NG HD NI NI NN NG NN NG NK NG; right TALEN monomer (2), NN HD NG NN NI NI NN HD NG NI HD NN NI HD NG NN HD HD; left TALEN monomer (3), NN NN NN NG NN NN HD NG NI NG NN NN HD NI NN HD HD NK; right TALEN monomer (4A), HD HD NG HD NG NG NN NN NI NN HD HD HD HD HD HD NI NK; right TALEN monomer (4B), NI NG HD HD NG HD NG NG NN NN NI NN HD HD HD HD HD HD.

Clonal Expansion

Transfected cells were detached from culture vessels with Accutase-100 (CELLnTEC) 7 days after incubation at 30°C for 3 days. Cells were counted using a hemocytometer and manually seeded using serial dilutions to obtain 1 cell/well of a 96-well plate. Immortalized human keratinocyte clones were co-cultured with 3T3-J2 mouse fibroblasts feeder cells (5–8 × 10^3 cells/cm^2) growth arrested with 4 μg/mL mitomycin C (Roche). Identified edited clones were detached from the surface of 96-well plates and transferred into 6-well plates with mitomycin C-treated feeders for further expansion.

T7 Endonuclease I Assay

Genomic DNA was isolated using phenol/chloroform extraction 1 week after transfection. The TALEN target site was PCR-amplified using Phusion polymerase (New England Biolabs) and analyzed by 0.8% agarose gel electrophoresis. The T7E1 assay for NKc21, EB11, EB21, and primary keratinocytes was performed as follows: forward primer 5′-CACCTCCCAACCCACTAGTG-3′ and reverse primer 5′-CCTTCCCAGCTGCCAGTCTA-3′ using 98°C for 30 s, 35 cycles of 98°C for 10 s, 65°C for 20 s, 72°C for 15 s, and 72°C for 7 min. Bands of corresponding size were extracted and purified using the GeneJET gel extraction kit (Thermo Scientific). The DNA fragments were then subjected to digestion with T7 endonuclease I (T7E1) (New England Biolabs). For the T7E1 assay, 200 ng of DNA was denatured at 95°C for 5 min, slowly cooled down to room temperature to allow the formation of heteroduplex DNA, treated with 5 U of T7E1 for 15 min at 37°C, and analyzed by 1.5% agarose gel electrophoresis. Quantification of gene disruption efficiency (as shown in Figure 2) was carried out according to Guschin et al.[53]

Genotyping

After reaching a sustainable size (>500 cells per clone) 10–200 cells of each clone were scraped off and collected using a 10-μL micropipette tip. TALEN target sites were analyzed by releasing genomic DNA from the collected cells using a Direct PCR kit (Thermo Scientific) according to the manufacturer's instructions, which was then amplified using Phusion polymerase (New England Biolabs). Direct PCR of EB11 clones was performed as follows: forward primer 5′-CACCTCCCAACCCACTAGTG-3′ and reverse primer 5′-CCTTCCCAGCTGCCAGTCTA-3′ using 98°C for 30 s; 35 cycles of 98°C for 10 s, 65°C for 20 s, and 72°C for 15 s; and 72°C for 7 min. Direct PCR of EB21 clones was performed as follows: forward primer 5′-CACCTCCCAACCCACTAGTG-3′ and reverse primer 5′-ACTTGGTGTCCAGAACCTTG-3′ using 98°C for 30 s; 35 cycles of 98°C for 10 s, 64°C for 20 s, and 72°C for 30 s; and 72°C for 7 min. PCR products of clones were analyzed by 0.8% agarose gel electrophoresis, and bands of the correct size were isolated, purified using GeneJET gel extraction kit (Thermo Scientific), and sequenced. Sanger sequencing was performed by Source Bioscience.

Allele-Specific PCR

WT and mutant alleles were analyzed by PCR amplification and sequencing using reverse primers binding to the point mutation or

WT sequence. Alleles of EB11 clones were amplified using Phusion polymerase (New England Biolabs). Alleles of EB21 clones were amplified using Taq polymerase (Thermo Scientific). For EB11, the following were used: forward WT primer 5′-TGCTCCACCAGG AACAAGCC-3′, forward mutant primer 5′-GCTCCAGGAACA AGCC-3′, reverse WT primer 5′-ACCTGCATTCCTCGCCCT-3′, and reverse mutant primer 5′-ACCTGCATTCCTCGCCCC-3′ 98°C for 30 s; 35 cycles of 98°C for 10 s, 71°C for 10 s, and 72°C for 1 min 20 s; and 72°C for 7 min. For EB21, the following were used: forward primer 5′-GCTCCACCAGGAACAAGCC-3′, reverse WT primer 5′-CTGCTCCAGGAACCGCAC-3′, and reverse mutant primer 5′-CTGCTCCAGGAACCGCAA-3′ 95°C for 3 min; 40 cycles of 95°C for 30 s, 62°C for 30 s, and 72°C for 1 min 20 s; and 72°C for 5 min. PCR products of alleles were analyzed by 0.8% agarose gel electrophoresis, and bands of the correct size were isolated, purified using the GeneJET gel extraction kit (Thermo Scientific), and sequenced.

Western Blotting

Total protein was extracted from cell cultures and electrophoretically separated and blotted as described previously.[54] For antigen detection, rabbit anti-K5 (AF138, Covance), 1:2,000, was used, and Coomassie staining was used to confirm equal loading. Horseradish peroxidase-conjugated species-specific secondary antibodies (Dianova) were used, and immunodetection was performed using Super Signal West Pico and Dura substrates (Pierce, Thermo Scientific). Densitometry ratios of each sample were calculated and presented as the fraction of change from the control expression value. The densitometry ratios from each sample were averaged (n = 3), and the data are presented as mean value ± SEM.

Stress Assay

Cells were cultured for 4 days to reach 80%–90% confluence as described below and subjected to stress. Cells were subjected to thermal stress as described previously.[9] Briefly, cells were transferred to a closed 43°C water bath for 30 min. Cells were then allowed to recover at 37°C for 15 min, followed by washing with PBS (without Ca^{2+} and Mg^{2+}), fixation, and immunocytochemistry. Cells were subjected to hypo-osmotic stress using urea (Sigma-Aldrich) as described previously.[55] Briefly, cells were immersed in medium containing 150 mM urea at 37°C for 5 min. Cells were then allowed to recover in normal tissue culture medium for 25 min, followed by washing with PBS, fixation, and immunocytochemistry. To assess the extent of IF abnormalities, the total number of cells and the number of cells containing cytoplasmic keratin aggregates for each condition were quantified by counting four different microscope fields on each coverslip. The results were expressed as a fraction (percentage) of the average total number of cells ± SEM.

Immunofluorescence

Cells were cultured in 12-well plates on glass coverslips in duplicates and fixed at −20°C with methanol for 5 min, followed by acetone for 20 s. K5 was stained with rabbit anti-K5 (AF138, Covance), 1:1,000, and goat anti-rabbit Alexa Flour 488-conjugated secondary antibody (Molecular Probes), 1:400. Nuclei were stained with DAPI. Immunofluorescence imaging was carried out using Zeiss Axio Imager II.

Live-Cell Imaging

Live-cell imaging was carried out using a total internal reflection fluorescence (TIRF) and spinning disk (Nikon) confocal microscope. Cells were cultured in 6-well plates for 4–5 days and subsequently locked in the microscope plate holder and covered with a holder lid 48 hr after transfection with an expression plasmid encoding EGFP-muK10 cDNA. The microscope chamber was maintained at 37°C in a 5% CO_2 humidified atmosphere. At the time of stress, the temperature of the plate holder and atmosphere was increased to 43°C for 30 min and quickly cooled to 37°C. Cells were visualized throughout the process up to 4 hr. Photographs were taken every 5 min at four fixed positions for each cell line or clone.

Off-Target Analysis

Potential off-target sites for *KRT5* TALENs were identified using TALE-NT 2.0.[56] Sites with the best alignments (lowest scores) and spacer lengths within the optimal spacer ranges (10–15 bp and 20–22 bp) were selected for analysis (Table S1). Genomic DNA was isolated using phenol/chloroform extraction 1 week after transfection. Off-target sites were amplified using GoTaq polymerase (Promega) with the corresponding primers (Table S2). Bands of corresponding size were extracted and purified using the GFX PCR DNA and gel band purification kit (GE Healthcare). The DNA fragments were then analyzed by T7E1 assay.

Ethics Statement

Written informed patient consent was obtained. Ethical approval was granted by the Newcastle and North Tyneside Research Ethics Committee and was sponsored by the Newcastle upon Tyne Hospitals National Health Service (NHS) Foundation Trust.

SUPPLEMENTAL INFORMATION

Supplemental Information includes eight figures and two tables and can be found with this article online at http://dx.doi.org/10.1016/j.omtm.2017.06.008.

AUTHOR CONTRIBUTIONS

Conceptualization, J.R.; Investigation, M.A. and U.K.; Resources, J.R.; Writing – Original Draft, M.A.; Writing – Review & Editing, J.R., U.K., T.C., and C.M.; Visualization, M.A.; Supervision, J.R. and C.M.; Funding Acquisition, J.R., T.C., and C.M.

CONFLICTS OF INTEREST

T.C. is a consultant for TRACR Hematology. All other authors declare no conflict of interest.

ACKNOWLEDGMENTS

This work was part of a self-funded studentship (to M.A.) and financially supported by DEBRA Austria (to U.K and J.R.) and grants from the German Federal Ministry of Education and Research (BMBF 01EO0803 to C.M. and T.C.). We are grateful to Thomas Lahaye

for kindly allowing us to use his TALEN Golden Gate cloning platform, Christien Bednarski for technical assistance in generating the TALENs, Hans Törmä for providing the immortalized keratinocyte lines, Ingo Haase for providing 3T3-J2 feeder cells, and Nick Reynolds and the Urology Department of the Freeman Hospital NHS Foundation Trust for providing primary keratinocytes. We thank Andrew Fuller and David McDonald from the Newcastle University Flow Cytometry Core Facility for help with flow cytometry. We also thank Alex Laude from the Newcastle University Bio-Imaging Unit for help with developing the live-cell imaging assay and Thorsten Höher for constructing the GFP-K10 plasmid. We also thank Jelena Mann for providing feedback and suggestions for the manuscript.

REFERENCES

1. Lee, C.H., and Coulombe, P.A. (2009). Self-organization of keratin intermediate filaments into cross-linked networks. J. Cell Biol. *186*, 409–421.
2. Szeverenyi, I., Cassidy, A.J., Chung, C.W., Lee, B.T., Common, J.E., Ogg, S.C., Chen, H., Sim, S.Y., Goh, W.L., Ng, K.W., et al. (2008). The Human Intermediate Filament Database: comprehensive information on a gene family involved in many human diseases. Hum. Mutat. *29*, 351–360.
3. Fuchs, E. (1995). Keratins and the skin. Annu. Rev. Cell Dev. Biol. *11*, 123–153.
4. Roshan, A., Murai, K., Fowler, J., Simons, B.D., Nikolaidou-Neokosmidou, V., and Jones, P.H. (2016). Human keratinocytes have two interconvertible modes of proliferation. Nat. Cell Biol. *18*, 145–156.
5. Letai, A., Coulombe, P.A., McCormick, M.B., Yu, Q.-C., Hutton, E., and Fuchs, E. (1993). Disease severity correlates with position of keratin point mutations in patients with epidermolysis bullosa simplex. Proc. Natl. Acad. Sci. USA *90*, 3197–3201.
6. Sørensen, C.B., Ladekjaer-Mikkelsen, A.-S., Andresen, B.S., Brandrup, F., Veien, N.K., Buus, S.K., Anton-Lamprecht, I., Kruse, T.A., Jensen, P.K., Eiberg, H., et al. (1999). Identification of novel and known mutations in the genes for keratin 5 and 14 in Danish patients with epidermolysis bullosa simplex: correlation between genotype and phenotype. J. Invest. Dermatol. *112*, 184–190.
7. Ishida-Yamamoto, A., McGrath, J.A., Chapman, S.J., Leigh, I.M., Lane, E.B., and Eady, R.A. (1991). Epidermolysis bullosa simplex (Dowling-Meara type) is a genetic disease characterized by an abnormal keratin-filament network involving keratins K5 and K14. J. Invest. Dermatol. *97*, 959–968.
8. Kitajima, Y., Inoue, S., and Yaoita, H. (1989). Abnormal organization of keratin intermediate filaments in cultured keratinocytes of epidermolysis bullosa simplex. Arch. Dermatol. Res. *281*, 5–10.
9. Chamcheu, J.C., Lorié, E.P., Akgul, B., Bannbers, E., Virtanen, M., Gammon, L., Moustakas, A., Navsaria, H., Vahlquist, A., and Törmä, H. (2009). Characterization of immortalized human epidermolysis bullosa simplex (KRT5) cell lines: trimethylamine N-oxide protects the keratin cytoskeleton against disruptive stress condition. J. Dermatol. Sci. *53*, 198–206.
10. Chamcheu, J.C., Virtanen, M., Navsaria, H., Bowden, P.E., Vahlquist, A., and Törmä, H. (2010). Epidermolysis bullosa simplex due to KRT5 mutations: mutation-related differences in cellular fragility and the protective effects of trimethylamine N-oxide in cultured primary keratinocytes. Br. J. Dermatol. *162*, 980–989.
11. Chamcheu, J.C., Navsaria, H., Pihl-Lundin, I., Liovic, M., Vahlquist, A., and Törmä, H. (2011). Chemical chaperones protect epidermolysis bullosa simplex keratinocytes from heat stress-induced keratin aggregation: involvement of heat shock proteins and MAP kinases. J. Invest. Dermatol. *131*, 1684–1691.
12. Rugg, E.L., McLean, W.H., Lane, E.B., Pitera, R., McMillan, J.R., Dopping-Hepenstal, P.J., Navsaria, H.A., Leigh, I.M., and Eady, R.A. (1994). A functional "knockout" of human keratin 14. Genes Dev. *8*, 2563–2573.
13. Chan, Y., Anton-Lamprecht, I., Yu, Q.C., Jäckel, A., Zabel, B., Ernst, J.P., and Fuchs, E. (1994). A human keratin 14 "knockout": the absence of K14 leads to severe epidermolysis bullosa simplex and a function for an intermediate filament protein. Genes Dev. *8*, 2574–2587.
14. Müller, F.B., Huber, M., Kinaciyan, T., Hausser, I., Schaffrath, C., Krieg, T., Hohl, D., Korge, B.P., and Arin, M.J. (2006). A human keratin 10 knockout causes recessive epidermolytic hyperkeratosis. Hum. Mol. Genet. *15*, 1133–1141.
15. Hickerson, R.P., Smith, F.J., McLean, W.H., Landthaler, M., Leube, R.E., and Kaspar, R.L. (2006). SiRNA-mediated selective inhibition of mutant keratin mRNAs responsible for the skin disorder pachyonychia congenita. Ann. N Y Acad. Sci. *1082*, 56–61.
16. Hickerson, R.P., Smith, F.J., Reeves, R.E., Contag, C.H., Leake, D., Leachman, S.A., Milstone, L.M., McLean, W.H., and Kaspar, R.L. (2008). Single-nucleotide-specific siRNA targeting in a dominant-negative skin model. J. Invest. Dermatol. *128*, 594–605.
17. Leachman, S.A., Hickerson, R.P., Schwartz, M.E., Bullough, E.E., Hutcherson, S.L., Boucher, K.M., Hansen, C.D., Eliason, M.J., Srivatsa, G.S., Kornbrust, D.J., et al. (2010). First-in-human mutation-targeted siRNA phase Ib trial of an inherited skin disorder. Mol. Ther. *18*, 442–446.
18. Atkinson, S.D., McGilligan, V.E., Liao, H., Szeverenyi, I., Smith, F.J., Moore, C.B., and McLean, W.H. (2011). Development of allele-specific therapeutic siRNA for keratin 5 mutations in epidermolysis bullosa simplex. J. Invest. Dermatol. *131*, 2079–2086.
19. Castanotto, D., and Rossi, J.J. (2009). The promises and pitfalls of RNA-interference-based therapeutics. Nature *457*, 426–433.
20. Tiemann, K., and Rossi, J.J. (2009). RNAi-based therapeutics-current status, challenges and prospects. EMBO Mol. Med. *1*, 142–151.
21. Kaspar, B.K., Roth, D.M., Lai, N.C., Drumm, J.D., Erickson, D.A., McKirnan, M.D., and Hammond, H.K. (2005). Myocardial gene transfer and long-term expression following intracoronary delivery of adeno-associated virus. J. Gene Med. *7*, 316–324.
22. Kim, H., and Kim, J.S. (2014). A guide to genome engineering with programmable nucleases. Nat. Rev. Genet. *15*, 321–334.
23. Cox, D.B., Platt, R.J., and Zhang, F. (2015). Therapeutic genome editing: prospects and challenges. Nat. Med. *21*, 121–131.
24. Rouet, P., Smih, F., and Jasin, M. (1994). Introduction of double-strand breaks into the genome of mouse cells by expression of a rare-cutting endonuclease. Mol. Cell. Biol. *14*, 8096–8106.
25. Barrandon, Y., and Green, H. (1987). Three clonal types of keratinocyte with different capacities for multiplication. Proc. Natl. Acad. Sci. USA *84*, 2302–2306.
26. Gallico, G.G., 3rd, O'Connor, N.E., Compton, C.C., Kehinde, O., and Green, H. (1984). Permanent coverage of large burn wounds with autologous cultured human epithelium. N. Engl. J. Med. *311*, 448–451.
27. Ronfard, V., Rives, J.M., Neveux, Y., Carsin, H., and Barrandon, Y. (2000). Long-term regeneration of human epidermis on third degree burns transplanted with autologous cultured epithelium grown on a fibrin matrix. Transplantation *70*, 1588–1598.
28. Mavilio, F., Pellegrini, G., Ferrari, S., Di Nunzio, F., Di Iorio, E., Recchia, A., Maruggi, G., Ferrari, G., Provasi, E., Bonini, C., et al. (2006). Correction of junctional epidermolysis bullosa by transplantation of genetically modified epidermal stem cells. Nat. Med. *12*, 1397–1402.
29. Bauer, J.W., Koller, J., Murauer, E.M., De Rosa, L., Enzo, E., Carulli, S., Bondanza, S., Recchia, A., Muss, W., Diem, A., et al. (2017). Closure of a large chronic wound through transplantation of gene-corrected epidermal stem cells. J. Invest. Dermatol. *137*, 778–781.
30. Höher, T., Wallace, L., Khan, K., Cathomen, T., and Reichelt, J. (2012). Highly efficient zinc-finger nuclease-mediated disruption of an eGFP transgene in keratinocyte stem cells without impairment of stem cell properties. Stem Cell Rev. *8*, 426–434.
31. De Luca, M., Pellegrini, G., and Green, H. (2006). Regeneration of squamous epithelia from stem cells of cultured grafts. Regen. Med. *1*, 45–57.
32. De Rosa, L., Carulli, S., Cocchiarella, F., Quaglino, D., Enzo, E., Franchini, E., Giannetti, A., De Santis, G., Recchia, A., Pellegrini, G., and De Luca, M. (2013). Long-term stability and safety of transgenic cultured epidermal stem cells in gene therapy of junctional epidermolysis bullosa. Stem Cell Reports *2*, 1–8.
33. Barrandon, Y., Grasset, N., Zaffalon, A., Gorostidi, F., Claudinot, S., Droz-Georget, S.L., Nanba, D., and Rochat, A. (2012). Capturing epidermal stemness for regenerative medicine. Semin. Cell Dev. Biol. *23*, 937–944.
34. Rochat, A., Grasset, N., Gorostidi, F., Lathion, S., and Barrandon, Y. (2013). Regeneration of epidermis from adult human keratinocytes stem cells. In Handbook of Stem Cells, A. Atala and R. Lanza, eds. (London: Academic Press), pp. 766–780.

35. Cornu, T.I., Mussolino, C., and Cathomen, T. (2017). Refining strategies to translate genome editing to the clinic. Nat. Med. *23*, 415–423.

36. March, O.P., Reichelt, J., and Koller, U. (2017). Gene editing for skin diseases: designer nucleases as tools for gene therapy of skin fragility disorders. Exp. Physiol. http://dx.doi.org/10.1113/EP086044.

37. Mussolino, C., Morbitzer, R., Lütge, F., Dannemann, N., Lahaye, T., and Cathomen, T. (2011). A novel TALE nuclease scaffold enables high genome editing activity in combination with low toxicity. Nucleic Acids Res. *39*, 9283–9293.

38. Mussolino, C., Alzubi, J., Fine, E.J., Morbitzer, R., Cradick, T.J., Lahaye, T., Bao, G., and Cathomen, T. (2014). TALENs facilitate targeted genome editing in human cells with high specificity and low cytotoxicity. Nucleic Acids Res. *42*, 6762–6773.

39. Chen, S., Oikonomou, G., Chiu, C.N., Niles, B.J., Liu, J., Lee, D.A., Antoshechkin, I., and Prober, D.A. (2013). A large-scale in vivo analysis reveals that TALENs are significantly more mutagenic than ZFNs generated using context-dependent assembly. Nucleic Acids Res. *41*, 2769–2778.

40. Bultmann, S., Morbitzer, R., Schmidt, C.S., Thanisch, K., Spada, F., Elsaesser, J., Lahaye, T., and Leonhardt, H. (2012). Targeted transcriptional activation of silent oct4 pluripotency gene by combining designer TALEs and inhibition of epigenetic modifiers. Nucleic Acids Res. *40*, 5368–5377.

41. Valton, J., Dupuy, A., Daboussi, F., Thomas, S., Maréchal, A., Macmaster, R., Melliand, K., Juillerat, A., and Duchateau, P. (2012). Overcoming transcription activator-like effector (TALE) DNA binding domain sensitivity to cytosine methylation. J. Biol. Chem. *287*, 38427–38432.

42. Barrandon, Y., and Green, H. (1985). Cell size as a determinant of the clone-forming ability of human keratinocytes. Proc. Natl. Acad. Sci. USA *82*, 5390–5394.

43. Coluccio, A., Miselli, F., Lombardo, A., Marconi, A., Malagoli Tagliazucchi, G., Gonçalves, M.A., Pincelli, C., Maruggi, G., Del Rio, M., Naldini, L., et al. (2013). Targeted gene addition in human epithelial stem cells by zinc-finger nuclease-mediated homologous recombination. Mol. Ther. *21*, 1695–1704.

44. Rochat, A., Kobayashi, K., and Barrandon, Y. (1994). Location of stem cells of human hair follicles by clonal analysis. Cell *76*, 1063–1073.

45. Mathor, M.B., Ferrari, G., Dellambra, E., Cilli, M., Mavilio, F., Cancedda, R., and De Luca, M. (1996). Clonal analysis of stably transduced human epidermal stem cells in culture. Proc. Natl. Acad. Sci. USA *93*, 10371–10376.

46. Mou, H., Vinarsky, V., Tata, P.R., Brazauskas, K., Choi, S.H., Crooke, A.K., Zhang, B., Solomon, G.M., Turner, B., Bihler, H., et al. (2016). Dual SMAD Signaling Inhibition Enables Long-Term Expansion of Diverse Epithelial Basal Cells. Cell Stem Cell *19*, 217–231.

47. Osborn, M.J., Starker, C.G., McElroy, A.N., Webber, B.R., Riddle, M.J., Xia, L., DeFeo, A.P., Gabriel, R., Schmidt, M., von Kalle, C., et al. (2013). TALEN-based gene correction for epidermolysis bullosa. Mol. Ther. *21*, 1151–1159.

48. Droz-Georget Lathion, S., Rochat, A., Knott, G., Recchia, A., Martinet, D., Benmohammed, S., Grasset, N., Zaffalon, A., Besuchet Schmutz, N., Savioz-Dayer, E., et al. (2015). A single epidermal stem cell strategy for safe ex vivo gene therapy. EMBO Mol. Med. *7*, 380–393.

49. Tebas, P., Stein, D., Tang, W.W., Frank, I., Wang, S.Q., Lee, G., Spratt, S.K., Surosky, R.T., Giedlin, M.A., Nichol, G., et al. (2014). Gene editing of CCR5 in autologous CD4 T cells of persons infected with HIV. N. Engl. J. Med. *370*, 901–910.

50. Chamcheu, J.C., Pihl-Lundin, I., Mouyobo, C.E., Gester, T., Virtanen, M., Moustakas, A., Navsaria, H., Vahlquist, A., and Törmä, H. (2011). Immortalized keratinocytes derived from patients with epidermolytic ichthyosis reproduce the disease phenotype: a useful in vitro model for testing new treatments. Br. J. Dermatol. *164*, 263–272.

51. Doyon, Y., Choi, V.M., Xia, D.F., Vo, T.D., Gregory, P.D., and Holmes, M.C. (2010). Transient cold shock enhances zinc-finger nuclease-mediated gene disruption. Nat. Methods *7*, 459–460.

52. Morbitzer, R., Elsaesser, J., Hausner, J., and Lahaye, T. (2011). Assembly of custom TALE-type DNA binding domains by modular cloning. Nucleic Acids Res. *39*, 5790–5799.

53. Guschin, D.Y., Waite, A.J., Katibah, G.E., Miller, J.C., Holmes, M.C., and Rebar, E.J. (2010). A rapid and general assay for monitoring endogenous gene modification. Methods Mol. Biol. *649*, 247–256.

54. Wallace, L., Roberts-Thompson, L., and Reichelt, J. (2012). Deletion of K1/K10 does not impair epidermal stratification but affects desmosomal structure and nuclear integrity. J. Cell Sci. *125*, 1750–1758.

55. D'Alessandro, M., Russell, D., Morley, S.M., Davies, A.M., and Lane, E.B. (2002). Keratin mutations of epidermolysis bullosa simplex alter the kinetics of stress response to osmotic shock. J. Cell Sci. *115*, 4341–4351.

56. Doyle, E.L., Booher, N.J., Standage, D.S., Voytas, D.F., Brendel, V.P., Vandyk, J.K., and Bogdanove, A.J. (2012). TAL Effector-Nucleotide Targeter (TALE-NT) 2.0: tools for TAL effector design and target prediction. Nucleic Acids Res. *40*, W117-22.